Platinum black electrodeposited thread based electrodes for dielectrophoretic assembly of microparticles

Renny Edwin Fernandez, Anil Koklu, Amin Mansoorifar, and Ali Beskok
Department of Mechanical Engineering, Southern Methodist University, Dallas, Texas 75205, USA

(Received 21 December 2015; accepted 13 March 2016; published online 11 April 2016)

We report dielectrophoretic (DEP) assembly of biological cells and microparticles using platinum-black electrodeposited conductive textile fiber. The three-dimensional conductive structures with high aspect ratios were found to facilitate high electric field regions, as revealed by scanning electron microscope characterization. The effective conducting area (A_{eff}) and its stability of thread electrodes were estimated using electrochemical methods. Potential of platinum black electrodeposited thread as 3-D electrodes for creating high gradient electrical field for dielectrophoretic assembly of microspheres and *Saccharomyces cerevisiae* (yeast cells) into 1D and two-dimensional structures over long ranges under the application of low voltages (4–10 V_{pp}) has been demonstrated. The formation of highly ordered pearl chains of microparticles using thread electrodes when subjected to dielectrophoresis (DEP) has been discussed in detail. *Published by AIP Publishing*. [http://dx.doi.org/10.1063/1.4946015]

I. INTRODUCTION

Conductive threads have been used in industry for a wide range of applications like wearable electronics and touch screen friendly apparels.[1,2] Thread has been utilized by researchers as a functional microfluidic element in qualitative and semi-quantitative immunoassays.[1,3–6] One of the most appealing features of thread based electrodes is its integrability into medical textile industry without having to overhaul the established practices of manufacturing. Properties like separation ability, fluid transport, three-dimensional (3D) geometry, enhanced surface area, light weight, and biocompatibility have attracted the researchers to consider thread as a strong alternative to the solid substrates.[3,5,6] Thread can also be effortlessly tailored into various flexible substrates like plastics or PDMS (Polydimethylsiloxane) for microfluidic flow and mixing applications.[5] Microfluidic components like flow valves and mixers have been developed with textile fibers by manipulating inter-fiber gaps and wicking properties of thread to increase or decrease its capillary driving ability of a liquid. Reches *et al*. improved the thread wicking properties by adopting different surface treatments for the detection of ketones, glucose, and proteins.[6] The separation ability and color displaying property of threads have been successfully applied to create bioassay platforms.[7] 3D microfluidic thread based devices have been developed by sewing cotton thread into polymer sheets to perform colorimetric assays.[1] Besides exploring the wicking properties of the thread, Nilgazh *et al*. demonstrated the effect of the microscale surface morphologies of thread on its separation efficiency of red blood cells.[8] By selecting thread with an appropriate surface morphology, a microfluidic device capable of accurately typing blood groups was built. Bhandari *et al*. showed that yarn parameters like twist frequency and weaving coverage area can be used to manipulate the wicking rate of a fabric.[9] Wei *et al*. developed a polyester thread based microfluidic system for low cost electrophoretic separation of mixed ion samples (Cl^-, Br^-, and I^-) using ferric cyanide salt as the redox molecule.[10] Sekar *et al*. recently fabricated a low-cost voltammetric sensor developed based on cellulose thread coated with screen-printing pastes for the detection of electro-active compounds.[11] Lu *et al*. developed a siphonage flow microfluidic thread based analytical device (S-μTAD) for the

detection of glucose and uric acid by covalently immobilizing the corresponding enzymes on cotton thread.[12] It has been reported that electrochemical detection of biosamples using thread based electrodes yields 10-folds current response than a conventional two-dimensional (2D) planar electrode.[13]

Despite all these developments, most of the above mentioned studies have explored only the physical and morphological characteristics of textile fibers for biomolecular separation or detection. For the first time, we demonstrate the potential of thread based electrodes in AC electrokinetic systems for developing cost-effective and disposable systems to analyze or separate microparticles and pathogens based on their dielectric properties. Polarizable microparticles in a liquid medium have been dielectrophoretically separated in a non-uniform AC electric field created by the porous 3D thread based electrodes. Unlike 2D planar electrodes, where strong dielectrophoresis (DEP) forces are confined only to the electrode's plain, a 3D electrode creates a more widespread and stronger electric field. 3D DEP trapping electrodes have shown to have a remarkable increase in cell trapping efficiency.[14] Effective conducting area of any electrode has been increased by electrodepositing platinum-black, which yields porous structures with high aspect ratio.[15–18] In the past, platinum-black electrodeposited microelectrodes have been used to develop micro-coulter-counter devices and implantable neuroprosthetics.[19–21]

In this work, we report the morphological and electrochemical characterization of platinum black electrodeposited thread and its application as 3D electrodes in dielectrophoretic capture and assembly of microspheres and biological cells. The electrochemical characterization of the microelectrodes was performed using cyclic voltammetry (CV) to compare the variation of active surface areas of threads with various thicknesses. Dielectrophoretic assembly of cells using thread can have a significant impact in wound care and drug delivery applications. Platelet aggregation, pathogen repulsion, dead cell removal, etc., are some of the likely areas where a thread based dielectrophoretic module can be integrated.

II. MATERIALS AND METHODS

Threads were purchased from Shieldex Trading, Inc. (Denier: 828, Nominal diameter: 0.2 mm). All chemicals used were of analytical grade and obtained from Sigma-Aldrich (St. Louis, USA). All solutions were prepared with 18 $M \cdot \Omega$ cm ultrapure water obtained from Millipore Alpha-Q water system (Bedford, MA, USA). Leo-Zeiss 1450VPSE variable pressure electron microscope equipped with an EDAX (Energy Dispersive Analysis of X-ray) Genesis 4000 XMS System was used for scanning electron microscope (SEM) characterization. SEM images were taken 60–5000× magnification factor at 30 kV resolution. Yeast cells (*Saccharomyces cerevisiae*) were grown in a shaking incubator at 30 °C and under constant shaking speed at 250 rpm. The growth medium (YEPD (Yeast Extract Peptone Dextrose) Broth) consisted of 20 g/l peptone, 10 g/l yeast extract, and 20 g/l dextrose dissolved in deionized (DI) water. The cells were collected at the stationary growth phase after 1 day of culture in shaking incubator, and they were harvested by centrifugation for 2 min at 3000 rpm, and re-suspended in measurement buffers. Plain polystyrene (PS) beads microspheres (10, 20 μm) were purchased from Polysciences, Inc., USA.

A. Electrodepostion and electrochemical characterization of platinum black on thread

A galvanostatic method of electrodeposition has been adopted for coating Platinum-black. A three-electrode system was used for electrochemical deposition. Ag/AgCl reference electrode and platinum wire counter electrode were operated with thread as working electrode within a plastic microfluidic channel made of lamination sheets with an exposed length of 5 mm. Platinum black was coated for 60, 140, 300, and 600 s at a current density of $-200\,mA/cm^2$. The electrolyte consists of 1% chloroplatinic acid and 0.08% lead acetate. The lead acetate strengthens the adhesion of Pt black on to the electrodes and also significantly enhances the electrode reactions in platinum black coating by mainly lowering the energy barrier for reduction of Pt (IV) to Pt (0) and by suppressing the reduction of Pt (IV) to Pt (II).[22,23] Coating conditions were optimized for both potentiostatic (−0.5 V) and galvanostatic conditions. The electroplated threads were immersed in 1M KOH for 24 h and thoroughly washed in DI water, following by a

2 min long oxygen plasma treatment for obtaining stable substrate.[24] Electrochemical measurements were performed using a four channel system (EZstat potentiostat and galvanostat, LabVIEW EZware software, Nuvant). The films were characterized between +0.800 and −0.500 V vs. Ag/AgCl in 2 mM $K_3[Fe(CN)_6] + 0.5$M KNO_3. Scan rates for characterization ranged from 0.020 V/s to 0.120 V/s.

B. COMSOL simulation

Numerical simulations of electric field in the micro-channels with planar electrodes and a representative thread geometry are solved using commercial finite element software COMSOL by applying ±1 V on the opposing electrodes. The resulting DEP force field is calculated assuming non-interacting point particles. The schematic drawings of the simulation domains for both cases are shown in Fig. S3 of the supplementary material with the three dimensional discretization of the domain using unstructured tetrahedral mesh.[35] Electrostatics equations are solved using an iterative solver (BiCGStab) with the convergence criteria of relative residual below 1×10^{-6}. The relative permittivity and conductivity of medium were taken as 80 and 5×10^{-6} S/m. Grid independence studies are performed by gradually increasing the number of elements. Numerical solution became grid independent approximately at 650 000 elements (Fig. S4[35]).

C. Dielectrophoretic capturing

Threads were arranged in a parallel fashion on glass substrates within patterned plastic microfluidic channels (Figs. 1(a)–1(c)). The electrodes were separated at a distance of 1 mm. All the measurements were performed using electric fields in the 1 kHz–40 MHz frequency range for all sets of electrodes. The experiments were conducted in DI water (5×10^{-6} S/m) and 1 mM KCl solution (0.01 S/m). Time averaged dielectrophoretic force generated by constant phase electric field is given by $\langle \bar{F}_{DEP} \rangle = 2\pi r^3 \varepsilon_0 \varepsilon_r Re[K(\omega)] \nabla E^2$, where r is the radius of particle, ε_0 represents the permittivity of vacuum, ε_r is the relative permittivity of the medium, ∇E^2 is the gradient of square of the electric field, and $Re[K(\omega)]$ is the real part of the Clausius-Mossotti factor which can be written as $K(\omega) = \frac{\varepsilon_p^* - \varepsilon_m^*}{\varepsilon_p^* + 2\varepsilon_m^*}$, where *, p, and m denotes complex value, particle, and medium, respectively. The complex permittivity is calculated $\varepsilon^* = \varepsilon - \frac{j\sigma}{\omega}$, where ε is the permittivity, σ is the conductivity, $j = \sqrt{-1}$, and ω is the angular frequency.

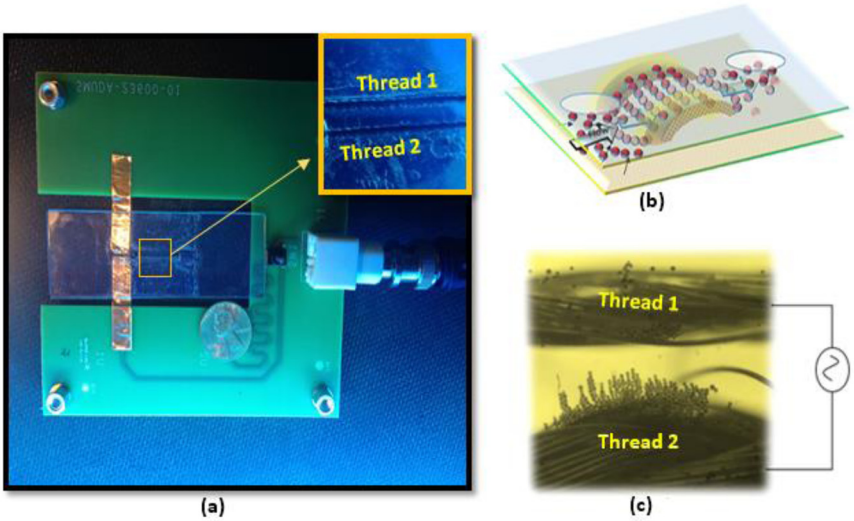

FIG. 1. (a) Construction of a two electrode thread configuration for on chip assembly of cells and microspheres. (b) Schematic of the two electrode configurations used for on-chip assembly of cell composites. (c) Example of dielectrophoretic assembly of PS microparticles (20 μm).

Particles exhibit either positive DEP (pDEP) or negative DEP (nDEP) depending on the sign of $Re[K(\omega)]$. Particles experiencing positive dielectrophoresis (pDEP) are attracted to high electric field regions, while particles that are less polarizable than the media are repelled to low electric field regions, and hence experience negative dielectrophoresis (nDEP).

III. RESULTS AND DISCUSSION

Platinum-black was deposited electrochemically on the conductive threads at a current density of 200 mA/cm^2 using 1% chloroplatinic acid and 0.08% lead acetate as electrolyte.[15,25] Under an optical microscope, platinum black appeared as a uniform black layer. The scanning electron microscope (SEM) pictures revealed a 2–3 μm thick sponge-like structure of deposited platinum black (Figs. 2(a)–2(h)). Many circular grains around 200–300 nm in diameter were observed. The threads were coated at varying times (120, 300, 600, and 900 s) in order to observe the effects of deposition time. At longer electrode deposition times, complex 3D clusters were observed that are expected to generate strong non-uniform electrical fields. Pretreatment of threads in oxygen plasma and KOH solution improved the hydrophilicity of substrates, which also helped in forming a uniform electrodeposited platinum black layer.[6,26] Stability of the electrodeposited threads was ensured by incubating them at 100 °C for 15 min followed by rinsing in DI water. Although temperature curing enhances the grain size and stability of the microstructures, it also causes a slight decrease in effective surface area.[27]

Morphological inclusions were observed on the thread surfaces even for 2 min electrodeposited samples. Figs. 2(a) and 2(b) show the morphology of a platinum black electrodeposited thread for 2 min at different magnifications. Slightly different morphologies were observed for higher electrodeposition times. Minute porous structures were observed on the thread as seen in Fig. 2(b). The electrodeposition was observed to create relatively uniform surfaces. The cluster sizes were found to be bigger for 5 min long electrodeposited samples as seen in Figs. 2(c) and 2(d). The grain sizes were found to be larger when deposition times were increased further. Ten minutes long electrodeposition gave rise to highly porous multilayer structures with more pronounced cauliflower-like structures (Figs. 2(e) and 2(f)). The structures were also found to extend across individual fibers to the adjacent fibers in the thread. Figs. 2(g) and 2(h) show the SEM micrographs for 15 min long depositions. The morphology of the structures had transformed from cauliflower-like to twiggy. This is possibly due to crumbling of the high aspect morphological inclusions notwithstanding the incubation and washing cycles.

A. Electrochemical characterization

Electrochemical stability of platinum-black coated threads was investigated with $K_3[Fe(CN)_6]$ redox probe. Typical cyclic voltammograms recorded in 2 mM $K_3[Fe(CN)_6] + 0.5$M KNO_3 of platinum-black electrodeposited threads at different scan rates are given in Fig. 3. In the range of 0.02–0.1 V/s, a linear relationship was observed between the peak current and the square root of scan rate, suggesting a diffusion controlled behavior. Peak current (I_p) values were found to increase with electrodeposition times (2–10 min). However, the CV of 15 min. electrodeposited samples was noisy and also yielded a higher peak potential separation (ΔE_p) value alluding to poor mass transport mechanism, which is in agreement with the SEM pictures. Effective surface area (A_{eff}) values were calculated using the Randles-Servick equation, $I_p = 2.65 \times 10^5 n^{2/3} A_{eff} D^{1/2} \upsilon^{1/2} C_0$, where n, D, and C_0 are the number of electrons transferred, diffusion coefficient, and concentration of the redox probe.[28] The I_p vs $\upsilon^{1/2}$ plot yielded a slope of $2.012 \times 10^{-4} A_{eff}\ \upsilon^{1/2}\ s^{1/2}$. By substituting the value of D and n, the A_{eff} was calculated to be 49.95×10^{-3} cm^2 for a five-ply thread (350 μm). The A_{eff} values were found to be 48.3×10^{-3} cm^2 for a three-ply thread (240 μm) and 42.55×10^{-3} cm^2 for a two-ply thread (180 μm). Although the thickness of the thread was reduced to half, the effective surface area had decreased only to about 16%. SEM pictures revealed the presence of larger sized structures on thinner threads which can be due to the fact that the electrodeposition was performed at constant current density regardless

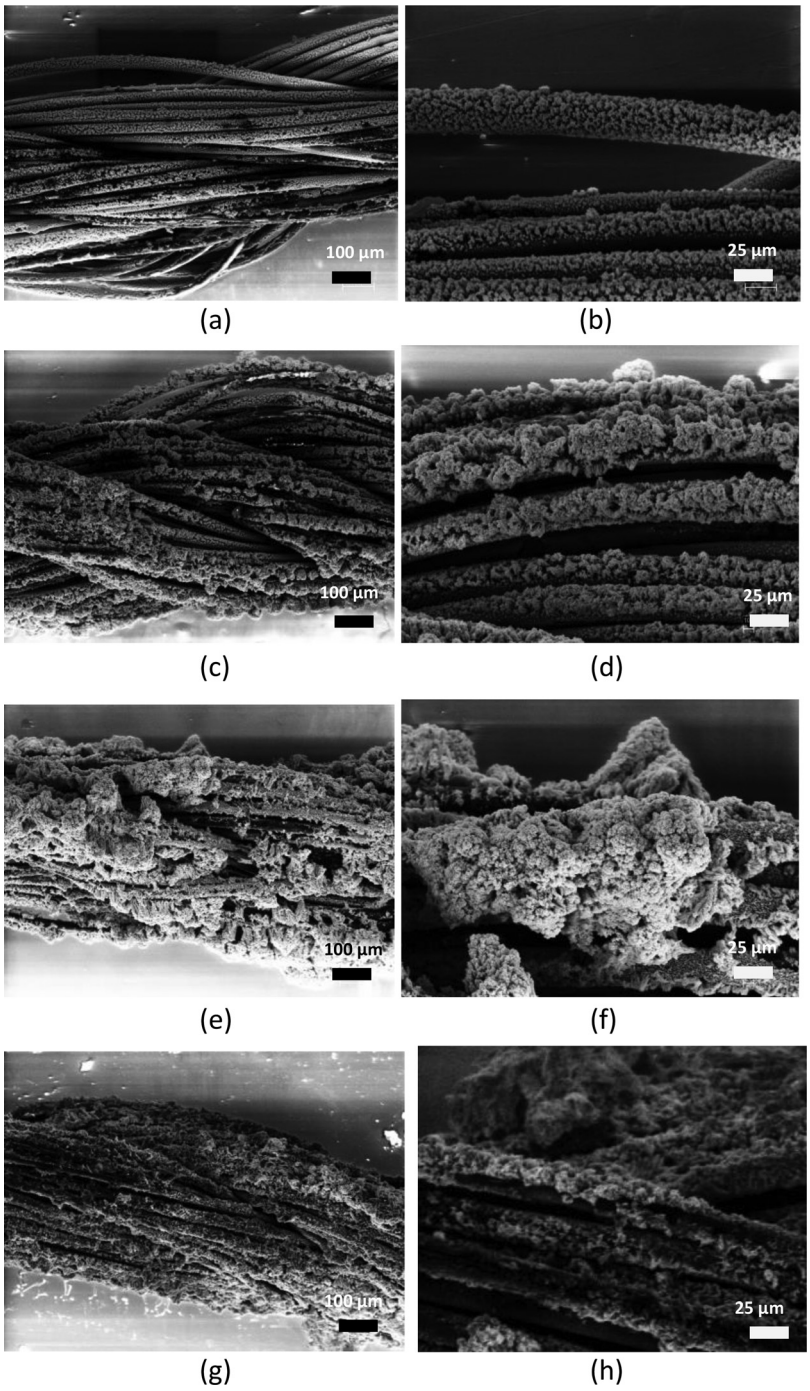

FIG. 2. SEM pictures of platinum black electrodeposited thread for (a) and (b) 2 min, (c) and (d) 5 min, (e) and (f) 10 min, and (g) and (h) 15 min. Electrochemical deposition was conducted at 200 mA/cm^2 using 1% chloroplatinic acid and 0.08% lead acetate platinum black solution.

of the thread thickness. Essentially, a non-complicated redox reaction suggested by cyclic voltammogram characterization established an electrochemically stable and diffusion controlled surface after platinum-black coating. However, stability of platinum-black coated threads depended on oxygen plasma pretreatment. CV curves revealed that untreated thread when subjected to electrodeposition yielded much lower values of I_p (Fig. S1[35]) in comparison with pretreated counterparts, signifying a much higher electron transfer rate.

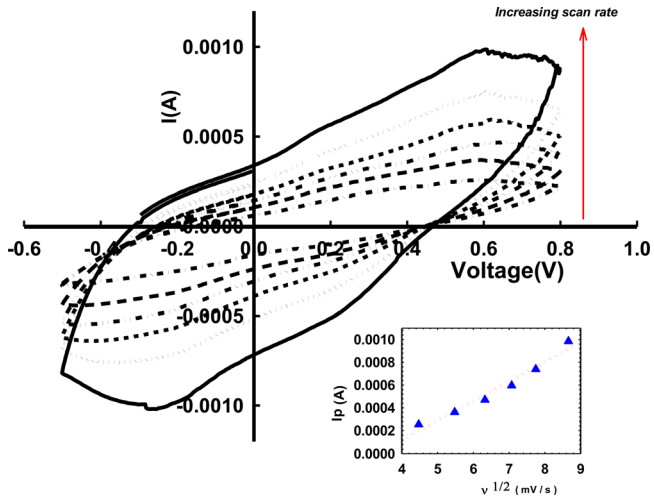

FIG. 3. Cyclic voltammetry for the reduction of 2 mM $K_3[Fe(CN)_6]$ at platinum black electrodeposited thread (thickness = 260 μm) at different scan rates (30, 40, 50, 80, 100, 120 mV/s). The effective surface area (A_{eff}) is obtained from Ip vs $\upsilon^{1/2}$ graphs (Inset).

1. Effect of 3D geometry on electric field

Electric field driven assembly of biological structures like tissues in their native morphologies has been performed in the past. Ho *et al*. have reported a DEP based cell patterning technique for on chip reconstruction of hepatic and endothelial cells using interdigitated electrodes.[29] However, cell patterning with interdigitated line electrodes generates poor electric field strengths. Well enhanced field gradients can be generated using 3D electrodes which are expensive to fabricate.[30]

Surface averaged DEP force (F_{DEP}) at different locations away from bottom of the channel is shown in Fig. 4. In the case of planar electrodes, the electrical field gradient in the vertical direction decays exponentially with distances away from the electrode surface and the DEP force becomes insignificant above 50 μm from the planar electrodes.[31] However, electrodes with extruding geometries were found to have an enhanced average DEP force (F_{DEP}). 3D electrodes generated an electric field that induced a dielectrophoretic force that is nearly an order of magnitude higher than the force generated by planar electrodes. Inset of Fig. 4 represents the electric field distribution considering thread as straight pillar geometry in a microfluidic channel. We notice that a 3D geometry induces a high value of F_{DEP} all along the width of the

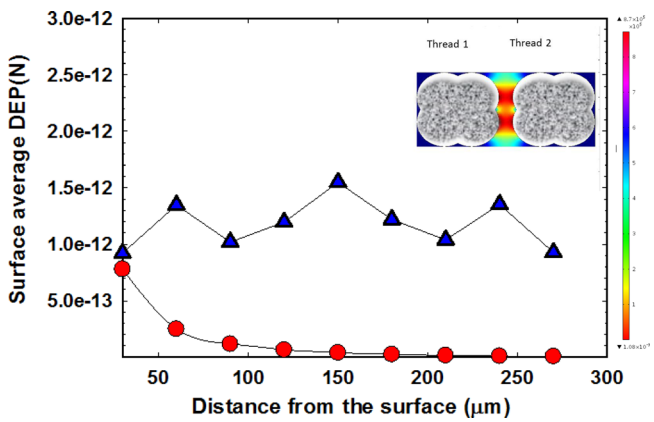

FIG. 4. Surface average DEP (F_{DEP}) force at different channel depths. Blue triangles represent the F_{DEP} at distances away from surface; red circles represent the F_{DEP} along the depth of the electrode with a 3D geometry. Inset shows the electric field distribution between 3D thread electrodes.

thread electrodes. The highest electric field was observed at locations where the separation between electrodes is least. Simulating the roughness of electrodeposited threads needs long computational time and cost and will be investigated extensively at a later time.

2. Dielectrophoretic assembly

The 3D structure of the thread electrodes was found to create regions of high electric fields that could rapidly assemble microspheres and biological cells at low voltages. Performance of thread electrodes in a DEP system was assessed by constructing electrodes with platinum black electrodeposited threads. DEP response of Polystyrene (PS) microparticles and *S, cerevisiae* cells was recorded using Olympus IX73 inverted microscope configured with RTC real time controller and Hamamatsu Orca Flash 4.0 SCMOS digital camera. Microparticle suspension was introduced into the microfluidic channel housing the electrodes.

Dielectrophoretic response of PS particles and yeast cells under AC electric fields can be theoretically modeled using solid-sphere and double-shell models, respectively.[32,33] Fig. S5[35] shows real part of the Clausius-Mossotti factor $(\mathrm{Re}[\mathrm{K}(\omega)])$ for yeast cells and PS microspheres as a function of frequency in 5×10^{-6} S/m and 0.01 S/m. Experiments were conducted at 250 kHz and 10 MHz for observing the dielectrophoretic behavior of cells and microspheres. According to the Clausius-Mossotti factor, yeast cells should exhibit pDEP at both test frequencies, while PS particles should exhibit pDEP at 250 kHz and nDEP at 10 MHz in both buffers.

At an applied voltage of 10 $V_{p\text{-}p}$ @ 250 kHz, we were able to aggregate microspheres (10–20 μm) within a gap as wide as 1 mm. Fig. 5 shows 15–20 μm PS microspheres displaying pDEP at 250 kHz, in agreement with the predictions from the Clausius-Mossotti factor. The response was extremely quick; the pearl chains start forming at edge of the threads within 3 s of the applied voltage. Due to local electric fields around them, the microspheres polarize and form pearl chains away from the electrodes, and length of the pearl chains rapidly increases with time at a constant applied voltage. Within 10 s, chains were aggregated at high electric field regions, which is a characteristic of pDEP. The pearl chains were loosely bound at the regions away from the electrode. Careful observations revealed that the aggregation is initiated by single particles getting attached to the thread surface likely on the platinum-black fractals (Fig. 5(b)). The pearl chains are formed in the low electric field region and are drawn towards the individual particles that are attached to the electrodes thus lengthening the chain. At higher volume fractions, there are lateral interactions between the PS particles and the pearl chains assemble into two-dimensional (2D) arrays (Fig. 5(c)). This behavior can be crucial in colloidal assembly, especially for wound healing. Fig. 6 depicts nDEP responses recorded for 10 μm PS microspheres at 10 $V_{p\text{-}p}$ and 10 MHz, 20 μm particles also showed similar behavior. From the figures, we can observe that the pearl chains are formed between the electrodes at low electric field regions, while nDEP response at this frequency pushes PS particles away from the thread electrodes.

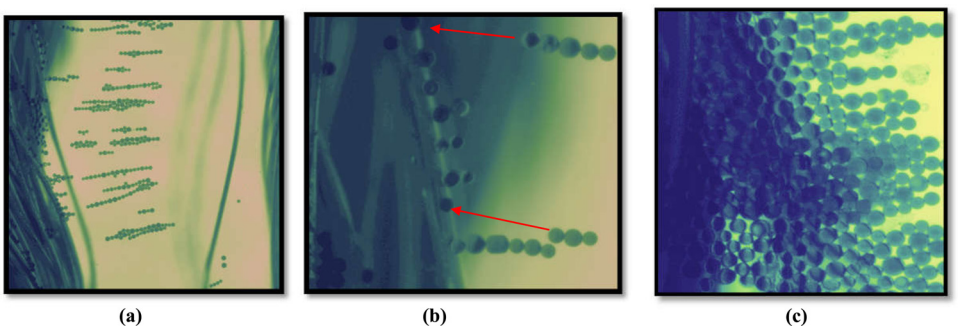

FIG. 5. Response of 15–20 μm PS microspheres to 10 V @ 250 kHz, t = 10 s. (a) Individual microspheres are attached to the high electric field regions. (b) Pearl chains are formed in the low electric field regions (away from the electrodes) and drawn towards the high electric field electrode regions. (c) At higher volume fractions, lateral interactions between the PS particles are noticed as the pearl chains assemble into 2D arrays.

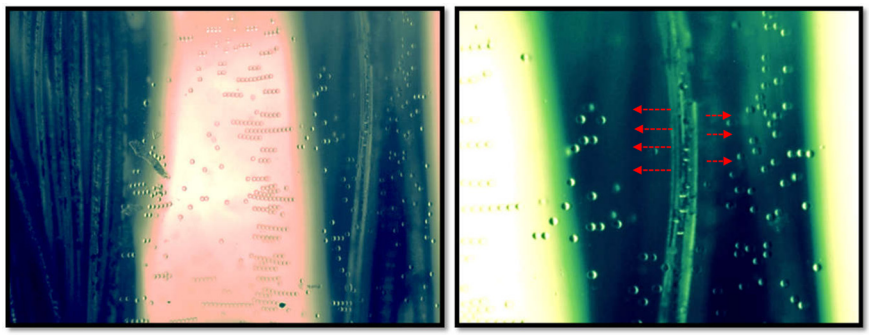

FIG. 6. Response of 10 μm PS microspheres to 10 V @ 10 MHz, t = 10 s. The particles are seen to form pearl chains in the low electric field regions away from the electrodes (a) and they are seen repelled from electrodes (b).

Experiments were conducted using yeast cells (*S. cerevisiae*). The yeast cells (7–10 μm) were found to instantly align themselves (within 2–3 s) to the electric field for 10 $V_{p\text{-}p}$ @ 250 kHz as seen in Fig. 7. Perpendicularly aligned threads (Fig. 7(c)) enable cells to move in a specific direction due to highly non-uniform electric fields. At relatively low voltages, single yeast cells were seen attached to the thread surface with no pearl chain extensions, as long range dipole interactions that facilitate directional assembly needs stronger electric fields.[29] However, comparing the DEP responses of PS microspheres and yeast cells, the most evident phenomena were the absence of lateral interactions between yeast cells. Even at extremely high concentrations, lateral interactions were absent for yeast cells which did not assemble into two-dimensional (2D) arrays (Fig. 7(d)). This may be attributed to its non-spherical shape, polydispersity, and weaker polarizability as reported in literature.[34]

The rate of aggregation and the strength of the pearl chains are affected by the applied voltage. It is preferable to assemble microparticles at lower voltages to avoid undesirable electro-thermal flows. Fig. 8(a) shows the assembly of microspheres at $4V_{pp}$ @ 250 kHz obtained using low volume fraction of PS particles. Microspheres assemble uniformly along the

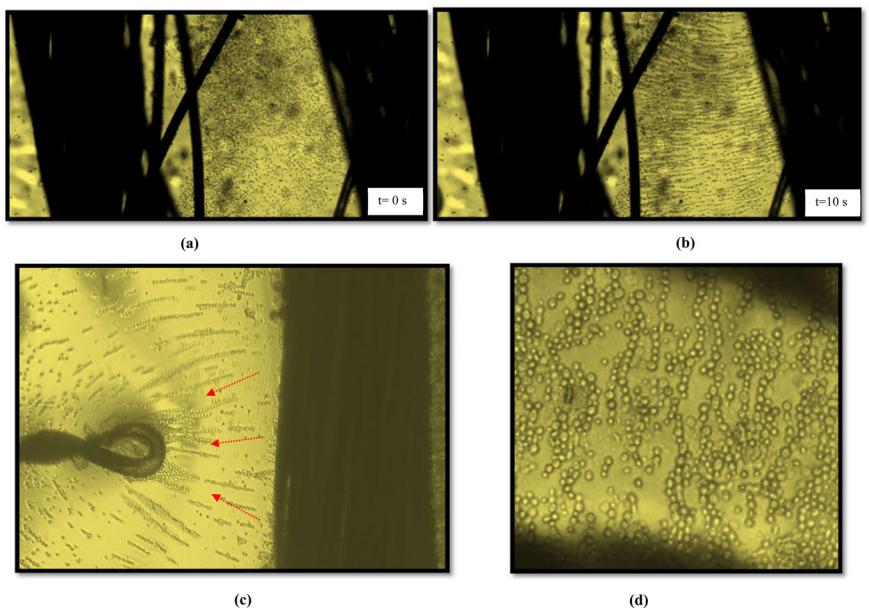

FIG. 7. (a) Thread based dielectrophoretic assembly: Response of 7–10 μm yeast cells to 10 V @ 250 kHz (a) t = 0 s, (b) t = 10 s, (c) perpendicularly aligned threads enables cells to move in a specific direction. (d) Assembly of yeast cells at high concentrations. (Multimedia view) [URL: http://dx.doi.org/10.1063/1.4946015.1]

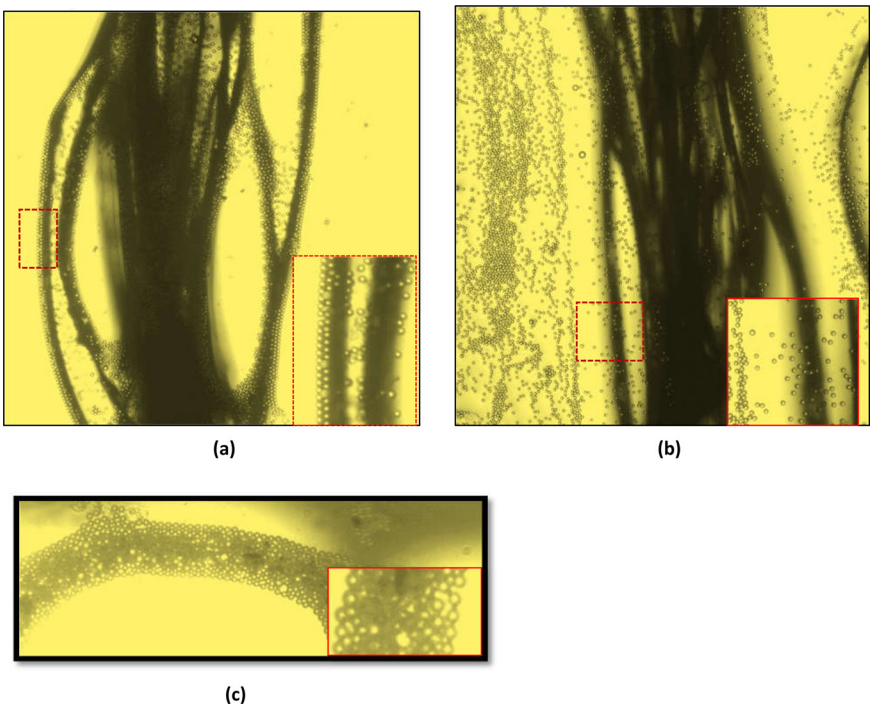

FIG. 8. Dielectric response of 10 μm PS microspheres to 4 V @ 250 kHz (a) and 10 MHz (b) in 10 s shows strong pDEP and nDEP, respectively. 2D lattice assembly of PS microspheres formed on the thread electrodes, drying after pDEP response (c).

edges of the thread, while long pearl chain extensions were completely absent in this case. At 10 MHz, the microparticles are instantly repelled from the thread due to the onset of nDEP as shown in Fig. 8(b). Both pDEP and nDEP forces could be generated with PS microspheres at voltages as low as 4 V_{pp} in 5×10^{-6} S/m and 0.010 S/m conductivity buffers. 2D lattice assembly of PS microspheres forming on the conductive thread electrodes after drying is shown in Fig. 8(c).

IV. CONCLUSION

We have reported the performance of platinum black electrodeposited thread as electrodes to generate strong electric fields for dielectrophoretic assembly of microspheres and biological cells. SEM characterization of electrodeposited conductive thread yielded cauliflower shaped porous structures with high aspect ratio. The electrochemical stability and effective surface area of the structures were estimated using cyclic voltammetry. Rapid assembly of microspheres and biological cells into highly ordered pearl chains has been presented.

We have demonstrated that thread based electrodes can be adopted for biological applications where rapid and uniform assembly of microparticles is necessary. Platelet and drug encapsulated microsphere distribution are some of the possible applications where a disposable, biodegradable electrode material like thread can be used for generating strong electric fields. Therefore, conductive threads can be incorporated into the textile materials and existing wound dressing applications such as bandage. We are currently exploring the possibilities of three dimensional assembly of microparticles using thread based electrodes for point-of-care applications.

[1]X. Li, J. Tian, and W. Shen, "Thread as a versatile material for low-cost microfluidic diagnostics," ACS Appl. Mater. Interfaces **2**(1), 1–6 (2010).
[2]J. Löfhede, F. Seoane, and M. Thordstein, "Textile electrodes for EEG recording—A pilot study," Sensors **12**(12), 16907–16919 (2012).

[3]D. R. Ballerini, X. Li, and W. Shen, "Flow control concepts for thread-based microfluidic devices," Biomicrofluidics **5**(1), 014105 (2011).
[4]X. Li, J. Tian, and W. Shen, "Progress in patterned paper sizing for fabrication of paper-based microfluidic sensors," Cellulose **17**(3), 649–659 (2010).
[5]X. Li, D. R. Ballerini, and W. Shen, "A perspective on paper-based microfluidics: Current status and future trends," Biomicrofluidics **6**(1), 011301 (2012).
[6]M. Reches, K. A. Mirica, R. Dasgupta, M. D. Dickey, M. J. Butte, and G. M. Whitesides, "Thread as a matrix for biomedical assays," ACS Appl. Mater. Interfaces **2**(6), 1722–1728 (2010).
[7]G. Zhou, X. Mao, and D. Juncker, "Immunochromatographic assay on thread," Anal. Chem. **84**(18), 7736–7743 (2012).
[8]A. Nilghaz, L. Zhang, M. Li, D. R. Ballerini, and W. Shen, "Understanding thread properties for red blood cell antigen assays: Weak ABO blood typing," ACS Appl. Mater. Interfaces **6**(24), 22209–22215 (2014).
[9]P. Bhandari, T. Narahari, and D. Dendukuri, "'Fab-Chips': A versatile, fabric-based platform for low-cost, rapid and multiplexed diagnostics," Lab Chip **11**(15), 2493–2499 (2011).
[10]Y. C. Wei, S. Y. Su, L. M. Fu, and C. H. Lin, "Electrophoresis separation and electrochemical detection on a novel line-based microfluidic device," in 25th IEEE International Conference on Micro Electro Mechanical Systems (MEMS) (2012).
[11]N. C. Sekar, S. A. M. Shaegh, S. H. Ng, L. Ge, and S. N. Tan, "Simple thick-film thread-based voltammetric sensors," Electrochem. Commun. **46**, 128–131 (2014).
[12]F. Lu, Q. Mao, R. Wu, S. Zhang, J. Du, and J. Lv, "A siphonage flow and thread-based low-cost platform enables quantitative and sensitive assays," Lab Chip **15**(2), 495–503 (2015).
[13]Y. A. Yang, Y. C. Wei, and C. H. Lin, "High performance thread-based CE-EC system with variable volume injection capability and 3D detection electrodes," in 9th IEEE International Conference on Nano/Micro Engineered and Molecular Systems (NEMS) (2014).
[14]N. Honda, M. Inaba, T. Katagiri, S. Shoji, H. Sato, T. Homma, T. Osaka, M. Saito, J. Mizuno, and Y. Wada, "High efficiency electrochemical immuno sensors using 3D comb electrodes," Biosens. Bioelectron. **20**(11), 2306–2309 (2005).
[15]C. A. Marrese, "Preparation of strongly adherent platinum black coatings," Anal. Chem. **59**(1), 217–218 (1987).
[16]R. Tang, W. Pei, S. Chen, H. Zhao, Y. Chen, Y. Han, C. Wang, and H. Chen, "Fabrication of strongly adherent platinum black coatings on microelectrodes array," Sci. China Inf. Sci. **57**(4), 1–10 (2014).
[17]M. Joncich and N. Hackerman, "Preparation and surface area measurements of platinized-platinum electrodes," J. Electrochem. Soc. **111**(11), 1286–1289 (1964).
[18]H. Oigawa, Y. Kirino, D. Yamazaki, and T. Ueda, "Quartz resonator hydrogen sensor using platinum black," in 5th International Conference on Sensing Technology (ICST) (2011).
[19]S. Zheng, M. Liu, and Y.-C. Tai, "Micro coulter counters with platinum black electroplated electrodes for human blood cell sensing," Biomed. Microdevices **10**(2), 221–231 (2008).
[20]N. Lago, K. Yoshida, K. P. Koch, and X. Navarro, "Assessment of biocompatibility of chronically implanted polyimide and platinum intrafascicular electrodes," IEEE Trans. Biomed. Eng. **54**(2), 281–290 (2007).
[21]S. A. Desai, J. D. Rolston, L. Guo, and S. M. Potter, "Improving impedance of implantable microwire multi-electrode arrays by ultrasonic electroplating of durable platinum black," Front. Neuroeng. **3**, 5 (2010).
[22]R. G. Bates, *Determination of pH: Theory and Practice* (Wiley Interscience Publication, 1973), ISBN: 9780471056478.
[23]M. Saitou, "Electrochemical characterization of platinum black electrodeposited from electrolyte including lead acetate trihydrate," Surf. Coat. Technol. **201**(6), 3611–3614 (2006).
[24]D. Malleo, J. Nevill, A. Van Ooyen, U. Schnakenberg, L. Lee, and H. Morgan, "Note: Characterization of electrode materials for dielectric spectroscopy," Rev. Sci. Instrum. **81**(1), 016104 (2010).
[25]A. Feltham and M. Spiro, "Platinized platinum electrodes," Chem. Rev. **71**(2), 177–193 (1971).
[26]C. Kim, M. R. Kendall, M. A. Miller, C. L. Long, P. R. Larson, M. B. Humphrey, A. S. Madden, and A. C. Tas, "Comparison of titanium soaked in 5M NaOH or 5M KOH solutions," Mater. Sci. Eng., C **33**(1), 327–339 (2013).
[27]B. Ilic, D. Czaplewski, P. Neuzil, T. Stanczyk, J. Blough, and G. Maclay, "Preparation and characterization of platinum black electrodes," J. Mater. Sci. **35**(14), 3447–3457 (2000).
[28]M. P. Siswana, K. I. Ozoemena, and T. Nyokong, "Electrocatalysis of asulam on cobalt phthalocyanine modified multi-walled carbon nanotubes immobilized on a basal plane pyrolytic graphite electrode," Electrochim. Acta **52**(1), 114–122 (2006).
[29]C. T. Ho, R. Z. Lin, R. J. Chen, C. K. Chin, S. E. Gong, H. Y. Chang *et al.*, "Liver-cell patterning Lab Chip: Mimicking the morphology of liver lobule tissue," Lab Chip **13**(18), 3578–3587 (2013).
[30]J. Voldman, M. Toner, M. Gray, and M. Schmidt, "Design and analysis of extruded quadrupolar dielectrophoretic traps," J. Electrostat. **57**(1), 69–90 (2003).
[31]C. Iliescu, G. Tresset, and G. Xu, "Dielectrophoretic field-flow method for separating particle populations in a chip with asymmetric electrodes," Biomicrofluidics **3**(4), 044104 (2009).
[32]Y. H. Su, M. Tsegaye, W. Varhue, K. T. Liao, L. S. Abebe, J. A. Smith *et al.*, "Quantitative dielectrophoretic tracking for characterization and separation of persistent subpopulations of Cryptosporidium parvum," Analyst **139**(1), 66–73 (2014).
[33]A. C. Sabuncu, J. Zhuang, J. F. Kolb, and A. Beskok, "Microfluidic impedance spectroscopy as a tool for quantitative biology and biotechnology," Biomicrofluidics **6**(3), 034103 (2012).
[34]S. Gupta, R. G. Alargova, P. K. Kilpatrick, and O. D. Velev, "On-chip dielectrophoretic coassembly of live cells and particles into responsive biomaterials," Langmuir **26**(5), 3441–3452 (2010).
[35]See supplementary material at http://dx.doi.org/10.1063/1.4946015 for thread DEP.